International Journal of Biochemistry and Cell Biology 107 (2019) 6–13

Contents lists available at ScienceDirect

International Journal of Biochemistry and Cell Biology

journal homepage: www.elsevier.com/locate/biocel

Impact of p38γ mitogen-activated protein kinase (MAPK) on MDA-MB-231 breast cancer cells using metabolomic approach

Hongshen Chen[a,b], Xin Wang[c], Fangdong Guo[b], Pisong Li[b], Dashuai Peng[d], Jianjun He[a,*]

[a] Department of Breast Surgery, The First Affiliated Hospital of Xi'an Jiaotong University, Xi'an, 710061, Shaanxi, China
[b] Department of Breast and Thyroid Surgery, Affiliated Zhongshan Hospital of Dalian University, Dalian, 116001, Liaoning, China
[c] Department of Nephrology, Affiliated Zhongshan Hospital of Dalian University, Dalian, 116001, Liaoning, China
[d] Urology Department One, The First Affiliated Hospital of Dalian Medical University, Dalian, 116011, Liaoning, China

ARTICLE INFO

Keywords:
Breast cancer
p38γ MAPK
MDA-MB-231 cell line
Metabolomics
Apoptosis

ABSTRACT

Background: The expression of p38 MAPK is high in breast cancer while its subunit p38γ had been rarely reported. We aimed to explain the effect of p38γ in breast cancer from the perspective of metabolomics.
Methods: In this study, we detected the expression of p38γ in 28 breast carcinoma and para-tumor samples. Following MDA-MB-231 cell transfection with p38γ siRNAs and pc-DNA-3.1, cell viability, apoptosis, metastasis were determined through CCK-8, the cytometry analysis, transwell assay and wound healing assay. Finally, gas chromatograph-mass spectrometer (GC–MS) was used for analysis the differential metabolites.
Results: The expression of p38γ was significantly up-regulated in breast cancer tissues. The transfection of si-p38γs could inhibit MDA-MB-231 cell propagation, metastasis, and induced cell apoptosis while overexpressed p38γ could promote the cell propagation, metastasis, and inhibit cell apoptosis. A total of 238 metabolites were identified and 72 of them differentially expressed in three groups (all $P < 0.05$, FDR < 0.05). Then the metabolites were enriched in the metabolism pathway, 85 pathways were included and 27 were significant (all $P < 0.05$, FDR < 0.05).
Conclusions: p38γ was up-regulated in breast cancer, which exerts a great influence on the cell growth, cell mobility, invasiveness, and apoptosis of MDA-MB-231 cells and also affected the metabolism.

1. Introduction

Breast cancer (BC) is one of the most prevalent tumors worldwide, accounting for 25% newly diagnosed cancers (Siegel et al., 2016). For Chinese women, BC is even the most frequently diagnosed cancer, and the occurrence of BC has been increasing in highly urbanized areas for the last decade (Fan et al., 2014). BC represents 25% of all cancer types in women, as the fifth most common cause of death (15%) (Smid et al., 2008). Breast cancer, similar to other cancers, occurs on the basis of a combination of various external factors and internal factors. For instance, women with *BRCA1/2* mutation are linked to a higher risk of BC (Antoniou et al., 2003; Kuchenbaecker et al., 2017) while long-term smoking also increases risk of BC (Johnson et al., 2011). The occurrence and development of BC is associated with environmental, life-style, genetic and hormonal factors (Dalasanur Nagaprashantha et al., 2018), which cause and sustain a wide range of alterations in metabolic network and signaling transduction as well. However, despite the tumor-intrinsic genomic aberrations, the molecular mechanisms of BC have not been fully elucidated yet. Identification of underlying mechanisms contributing to carcinogenesis may reveal novel cancer targets for drugs and thus provide new optimized BC therapies.

Mitogen-activated protein kinases (MAPKs) pathway, among the most thoroughly studied signaling pathways, function as the regulators of a series of cellular processes relevant to tumorigenesis and cancer development, including differentiation, propagation, inflammation, apoptosis, survival and innate immunity (Kim and Choi, 2015). The p38 MAPK is one of the three major MAPK cascades, and it was reported that Jun N-terminal kinase (JNK) and p38 MAPK signaling was involved in cancers in both humans and mice (Wagner and Nebreda, 2009). Furthermore, a study by Davidson et al. showed that the elevated JNK and p38 activation in breast carcinoma effusions may contribute to the survival of BC cells rather than apoptosis (Davidson et al.,

Abbrevations: BC, breast cancer; GC–MS, gas chromatograph–mass spectrometer; JNK, Jun N-terminal kinase; MAPKs, mitogen-activated protein kinases; MMCA, metabolite-metabolite correlation analysis; PC, primary component; shRNA, small hairpin; UV, ultraviolet ray

* Corresponding author at: Department of Breast Surgery, The First Affiliated Hospital of Xi'an Jiaotong University, No.277 Yanta West Road, Xi'an 710061, Shaanxi, China.
E-mail address: chinahjj@163.com (J. He).

https://doi.org/10.1016/j.biocel.2018.11.002
Received 25 April 2018; Received in revised form 1 November 2018; Accepted 6 November 2018
Available online 14 November 2018
1357-2725/

2006). Nevertheless, p38γ (also called stress-activated protein kinase 3 or ERK6), as an isoform of p38 MAPK, has not been well-studied. Previous studies revealed that p38γ protein was highly expressed in several human malignant cell lines (Pramanik et al., 2003) and p38γ was proved to enhance invasion in BC (Qi et al., 2006), suggesting its probable effective role in cancer development and p38γ integrates signals of Ras and estrogen receptor to enhance invasion in BC (Qi et al., 2006). P38γ has also been proved that it can affect the cellular morphology in the previous study (Al-Mahdi et al., 2015). Therefore, we sought to illuminate the role of p38γ in MDA-MB-231 Breast Cancer Cells.

It is widely accepted that signaling pathway can regulate and interact with metabolism. Consequently, aberrant signaling transduction will cause metabolic perturbation concurrently. Natalia et al. demonstrated that the activation of p38α could lead to increased glucose oxidation and fatty acid synthesis (Trempolec et al., 2017) while p38γ/δ was reported to regulate triglyceride and glucose metabolism in liver (Gonzalez-Teran et al., 2016). Given a systemic metabolic impact of p38γ MAPK on BC, a metabolomic approach, as a powerful tool for investigating metabolism at a global level, is utilized in our study. Metabolomics is one of the emerging omic sciences, aiming at the comprehensive characterization of metabolites and various metabolism in biological systems (Wishart, 2016), which can provide information for understanding disease mechanisms and to be more specific, how p38γ influenced metabolism in BC in our study. Gas chromatography-mass spectrometry (GC–MS) was applied for metabolite profiling due to the availability of GC–MS libraries for rapid identification of different metabolites in complicated biospecimen (Schauer et al., 2005).

This study was designed to explore the effect of p38γ on BC cells via an established metabolic profile. By elucidating the role of p38γ that it assumed and the influenced metabolism in BC, essential insights into the intercellular environment and distinction of tumor and para-tumor sample related with p38γ can be provided for the discovery of new drugs targeting at p38γ, as novel therapies for BC. Additionally, our study may contribute to delineation of the biochemical mechanisms of BC molecularly and metabolically.

2. Materials and methods

2.1. Clinical specimens

Breast cancer and para-tumor tissues from 28 patients at The First Affiliated Hospital of Xi'an Jiaotong University were collected in the period between 2015 and 2017. The study data of patients are shown in Table 1. The samples were fresh frozen and reserved at −80 °C. This study was approved by The First Affiliated Hospital of Xi'an Jiaotong University.

Table 1
The characteristics of patients.

Characteristics	Summary
Age (Mean ± SD)	53.8 ± 15.2
Grade	
I	3
II	10
III	13
NA	2
Node status	
N0	15
N1	2
N2	6
N3	3
NA	2

SD: Standard Deviation.

2.2. Immunohistochemistry

The tissues were harvested in 4% formaldehyde buffer containing phosphate-buffered saline, embedded in paraffin and then sectioned. An antibody against p38γ (#AF1347,10 μg/ml R&D Systems, Inc., Minneapolis, USA) was used for immunohistochemical analyses. Immunoreactivity was detected using a horseradish peroxidase (3,3′-diaminobenzidine substrate) kit (BioGenex), followed by slides counterstained with hematoxylin, dehydrated and mounted. The sections were ultimately evaluated under the optical microscopy.

2.3. qRT-PCR

PureLink RNA Mini Kit (Invitrogen, Carlsbad, CA, USA) was used to extract the total RNA from BC tissues and cell lines. The detailed procedure was in accordance with the manufacture's protocols. PCR was then conducted on MiniOpticon real-time PCR system (Bio-Rad, Hercules, CA, USA). Relative expression of p38γ was measured by $2^{-\Delta\Delta Ct}$ method. PCR primers were synthesized by Sangon Biotech (Shanghai, China) and the primer was as followed: p38γ sense sequence 5′- GGCATCCATCAGAGCAGAC-3′; p38γ antisense sequence 5′- GTCT GCTCTGATGGATGCC-3′; GAPDH Forward: 5′-CTGTTCGACAGTCAGC CGCATC-3′; GAPDH Reverse: 5′-GCGCCCAATACGACCAAATCCG-3′ was used as the internal reference. All the experiments were repeated 3 times.

2.4. Protein extraction and western blotting

The cell apoptosis was evaluated using flow cytometry. Total protein extraction was conducted following the instructions of kits from Shanghai Gefan Biotechnology Co. Ltd, followed by the quantification of protein concentrations using BCA assay with BSA standards (Pierce/Thermo). After separating on a 10% SDS-PAGE, proteins were shifted onto PVDF membranes. Membranes were blocked by 5% nonfat milk in Tris-buffered saline Tween (TBST). Membranes were incubated with p38γ primary antibodies (0.2 μg/ml) overnight at 4 °C and then washed in TBST and incubated with the appropriate horseradish peroxidase-labeled secondary antibodies for 1 h. Afterward, membranes were incubated with electrochemiluminescence (ECL) substrate for horseradish peroxidase (Pierce/Thermo), and the ECL intensity was detected by x-ray film exposure in a dark room by the SRX-101 A medical film processor (Konica Minolta, Mississauga, Ontario, Canada). The expression levels of proteins as indicated by the ECL intensity were measured with Image *J* software (Bethesda, MD, USA).

2.5. Cell culture

Human breast cancer cell line MDA-MB-231 and human mammary epithelial cell line MCF-10 A were procured from BeNa Culture Collection Biological Technology Co., Ltd. (Beijing, China). The cells were cultured in DMEM/high glucose medium (Gibco) plus 10% FBS (Gibco, Carlsbad, CA, USA), penicillin (100 U/ml) and streptomycin (100 μg/ml) (Xinfan, Nanjing, China). Cells were incubated at 37 °C in a humidified chamber supplemented with 5% CO_2.

2.6. Transfection of small hairpin interference RNA

p38γ shRNA plasmid and pc-DNA-3.1-p38γ for human were obtained from Santa Cruz Biotechnology (sc-39013-SH). Both cells were placed in 60-mm dishes (6×10^5 cells each dish). They were co-transfected after plating with p38 shRNA and pc-DNA-3.1-p38γ at 1 μg per dish via Lipofectamine 2000 for 2 days. Puromycin at a final concentration (0.5 μg/ml) was complemented to the culture medium on the 3rd day after transfection and then purely transfected cells were collected.

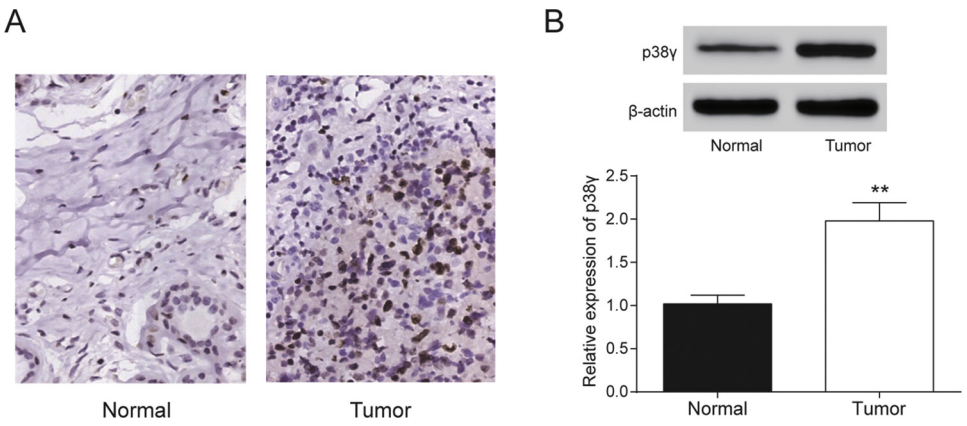

Fig. 1. Expression of p38γ in breast cancer tissue.
(A) IHC assay showed that p38γ appeared positive cell nucleus. (B) Western blot was conducted to measure the relative level of p38γ protein. * $P < 0.05$, compared with control group.

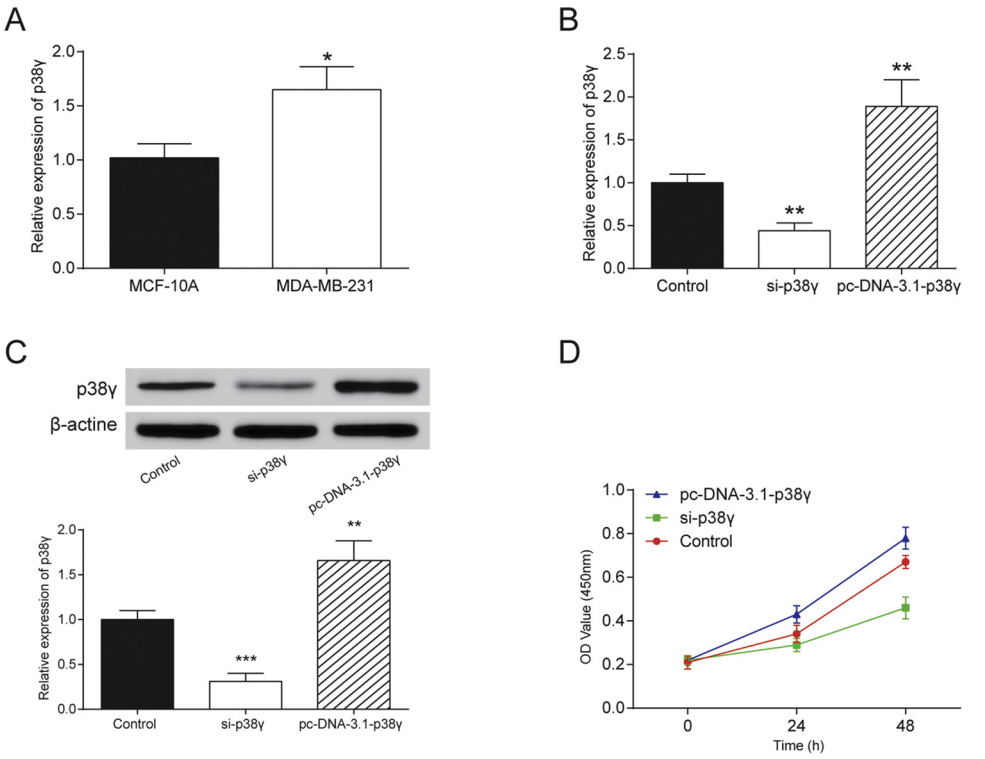

Fig. 2. The expression and the viability of p38γ. (A) The expression of p38γ in normal breast cell line and breast cancer cell lines by qRT-PCR. (B) The expression of p38γ after transfection, which indicated that the transfection was successful. (C)Protein expression of p38γ detected using Western Blot. (D) Cell viability was detected using CCK-8 assay. * $P < 0.05$ versus control group, ** $P < 0.01$ versus control group, *** $P < 0.01$ versus control group.

2.7. Cell viability assay

The impact of p38γ on cell viability was examined using CCK-8 assay. Transfected cells were seeded in flat-bottom and cultured in an adapt circumstance at 37 °C following the Cell Counting Kit-8 instructions from Dojindo Molecular Technologies Inc. The cells were harvested at 0 h, 24 h and 48 h, timing started when the cells adhered to the wall. Subsequently, OD values were analyzed using Synergy H4 Hybrid ELIASA (Biotek Winooski, Vermont, USA) at 450 nm.

2.8. Flow cytometric (FCM) analysis

Cells were digested using 0.25% pancreatic enzymes and suspended into single cell suspension after transfection overnight. Next, the cells were centrifuged (1000 rpm/min) and collected, and then washed twice with PBS and fixed with 70% ethyl alcohol overnight at −20 °C. Thereafter, the cells were resuspended in 1 ml of PBS. The cells were then stored in dark for 30 min and then stained with the Annexin V-FITC/PI Apoptosis Detection Kit (Beyotime, Shanghai, China).

2.9. Transwell invasion assay

A 8 μm-pore Transwell chamber (Corning, Cambridge, MA, USA) was used. After 24 h of transfection, 200 μl of a non-serum cell suspension was placed into the upper chambers covered with 50 μl Matrigel (1:4, BD Biosciences). The lower chamber was complemented with 500 μl DMEM containing 10% FBS. Following 24 h incubation, the cells on the upper surface were removed, whereas the invaded cells on the lower surface were immobilized and stained with 0.1% crystal violet for half an hour. The above experiments were carried out three times.

2.10. Wound healing assay

1×10^5 cells were seeded in 6-well plates after transfection. A wound line with was drawn on the layer using 1 μl pipettes' spearhead

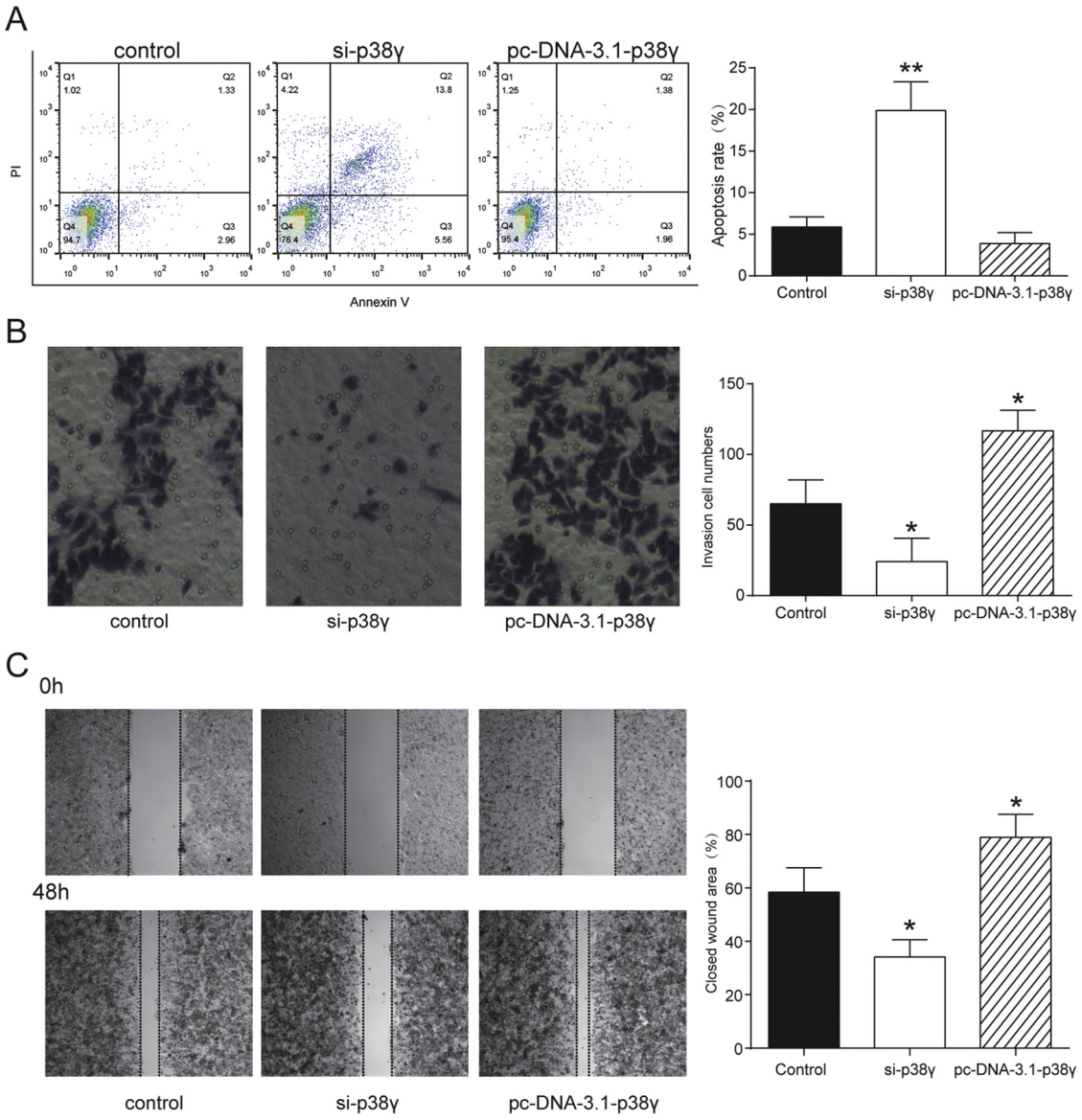

Fig. 3. Effects of p38γ on the apoptosis, invasion and migration of MDA-MB-231 cell line. (A) Cell apoptosis was detected using flow cytometry. (B) Cell invasion was detected using Transwell assay. (C) Cell migration was detected using wound healing assay. Data were presented as mean ± SD for three independent experiments. * $P < 0.05$ versus control group, ** $P < 0.01$ versus control group, *** $P < 0.01$ versus control group.

on the second day. The cells were rinsed twice in PBS and then incubated overnight in a serum-free culture medium. The number of migratory cells in every group was counted 48 h after the incubation, respectively.

2.11. Sample preparation for GC–MS analysis

The cells were washed with 0.9% NaCl three times after medium. Cells were frozen in liquid nitrogen before storage at -80 ℃. Next, 400 µl internal standards plus 40 nmol ribitol were complemented to the cells, followed by adding 10 ml of ice-cold methanol, removing the cells and shifting into a 50 ml Falcon tube. The plate was rinsed using 10 ml of ice-cold distilled water, and then the suspension was shifted into the same Falcon tube supplemented with 2 ml chloroform. Samples were vortexed for 1 min to favor extraction and then incubated for 15 min and then underwent centrifugation at 4000 rpm for 5 min. The aqueous-methanolic phase was segregated and shifted into a different Falcon tube and maintained at −80 ℃. 90 µL MSTFA (Sigma-Aldrich) was complemented into samples, which were then incubated at 37 ℃ prior to centrifugation at 14,000 rpm for 5 min. The supernatant was shifted to an auto sampler vial for GC–MS analysis. Finally 10 µl of 1 mM 2-fluorobiphenyl (in anhydrous pyridine) was added to the samples as an injection standard.

2.12. GC–MS analysis

GC–MS analysis was conducted on a TSQ8000 Triple Quadrupole GC–MS (Thermo Fisher Scientific) equipped with a TG-5MS capillary column and samples were processed through electron ionization at 70 eV. The GC was programed with an injection temperature (250 ℃) and splitless injection volume (2 µl). The starting temperature of GC oven program was set as 100 ℃ for 1 min, soaring to 250 ℃ in 5 ℃/min rate for 6 min. The GC flow rate with helium carrier gas was 1.2 ml/min. Identified metabolites were measured through the total ion count peak area. The mean, standard deviation, and 95% confidence interval were calculated for each group.

Table 2
The differential metabolites identified by GC–MS among three groups.

Metatbolites	P.value	FDR
Adenosine	6.03E-14	1.44E-11
Methylparaben	1.28E-11	1.52E-09
Ophthalmic acid	3.52E-11	2.79E-09
Glutathione	1.29E-10	6.16E-09
Lumichrome	1.05E-10	6.16E-09
3-Methyladenine	1.77E-10	7.03E-09
Adenine	5.85E-10	1.99E-08
Phosphocreatine	6.94E-10	2.06E-08
Spermine	1.47E-09	3.89E-08
Glycero-3-phosphocholine	2.44E-09	5.81E-08
5'-Methylthioadenosine	2.70E-09	5.84E-08
Uridine	3.36E-08	6.66E-07
S-Adenosylhomocysteine	1.28E-07	2.34E-06
GDP-glucose	2.41E-07	4.10E-06
Dithiodivaline	2.98E-07	4.72E-06
NAD	4.08E-07	5.89E-06
Pantothenic acid	4.21E-07	5.89E-06
Adenosine diphosphate ribose	5.24E-07	6.93E-06
Sphinganine	1.30E-06	1.63E-05
2'-Deoxyguanosine 5'-monophosphate	1.38E-06	1.65E-05
S-Adenosylmethionine	1.45E-06	1.65E-05
Adenosine monophosphate	1.68E-06	1.80E-05
DL-*O*-Phosphoserine	1.74E-06	1.80E-05
D-Galactose	3.52E-06	3.49E-05
Pentopyranose	5.29E-06	5.04E-05
L-Cystine	6.95E-06	6.36E-05
Inosine	7.32E-06	6.45E-05
Serotonin	9.67E-06	8.22E-05
Galactitol	1.09E-05	8.96E-05
Nicotinic acid adenine dinucleotide	1.19E-05	9.47E-05
N-Acetylputrescine	1.78E-05	1.37E-04
Docosahexaenoic acid	2.15E-05	1.60E-04
*n*_acetyl_*d*_hexosamine	3.12E-05	2.25E-04
N-Acetyl-L-methionine	3.89E-05	2.72E-04
3-Hydroxyphenylacetic acid	4.16E-05	2.83E-04
BOC-LYS-OH	5.68E-05	3.75E-04
Deoxyadenosine	6.92E-05	4.45E-04
6-Phosphogluconic acid	1.09E-04	6.83E-04
Pyridoxal	2.62E-04	1.60E-03
Ketoleucine	3.24E-04	1.93E-03
SM(d18:1/18:0)	3.71E-04	2.15E-03
Glycine	4.27E-04	2.42E-03
boc_phe_oh	6.69E-04	3.70E-03
Ortho-Hydroxyphenylacetic acid	7.88E-04	4.26E-03
Spermidine	8.50E-04	4.40E-03
L-Tryptophan	8.37E-04	4.40E-03
5'-Deoxyadenosine	9.62E-04	4.87E-03
Cyclic AMP	1.86E-03	9.17E-03
ARG-VAL-TRP	1.89E-03	9.17E-03
Shikimic acid	2.11E-03	1.00E-02
Cytidine 2',3'-cyclic phosphate	2.26E-03	1.05E-02
3-CMP	2.41E-03	1.10E-02
Fructose 1,6-bisphosphate	2.52E-03	1.13E-02
BOC-ASP-OH	3.02E-03	1.33E-02
4-Guanidinobutanoic acid	4.15E-03	1.79E-02
Guanosine monophosphate	4.76E-03	2.02E-02
1_Oleoyl_Rac_Glycerol	5.06E-03	2.11E-02
N-Acetyl-L-aspartic acid	6.14E-03	2.52E-02
ADP	7.54E-03	3.04E-02
Sorbic acid	8.13E-03	3.23E-02
Urocanic acid	8.42E-03	3.29E-02
Dihydroxyacetone phosphate	8.93E-03	3.43E-02
dGDP	1.02E-02	3.73E-02
Citric acid	1.01E-02	3.73E-02
Hypotaurine	1.03E-02	3.73E-02
Methyl Jasmonate	1.02E-02	3.73E-02
Pyridoxal 5'-phosphate	1.06E-02	3.76E-02
L-Arginine	1.13E-02	3.94E-02
4,5-Dihydroorotic acid	1.23E-02	4.23E-02
N6,N6,N6-Trimethyl-L-lysine	1.24E-02	4.23E-02
Phosphorylcholine	1.32E-02	4.43E-02
5-Hydroxyindoleacetic acid	1.45E-02	4.80E-02

FDR: False discovery rate.

2.13. Statistical analysis

Data were analyzed using SPSS 21.0 software (IBM, Armonk, NY, USA) and GraphPad Prism 6.0 (Version X; La Jolla, CA, USA), and recorded as mean ± standard deviation (SD). Comparison between two groups was evaluated through *Student t-test*, and statistically significanc hinged on $P < 0.05$. Metaboanalysis 3.0 (http://www.metaboanalyst.ca) online software was applied to data visualization, heatmap, PLS-DA construction, enriched pathway and correlation analysis.

3. Result

3.1. Expression of p38γ in BC tissues

Western blot assay revealed that the expression of p38γ in BC tissues was up-regulated in contrast to the expression of para-tumor tissues ($P < 0.05$). The result was indicated by immunohistochemistry and Western Blot (Fig. 1A-B).

3.2. Si-p38γ suppresses breast cancer cells viability and promotes apoptosis

The expression of p38γ was higher in MDA-MB-231 cell lines compared to MCF-10 A cell lines (Fig. 2A). The expression of p38γ decreased significantly in si-p38γ group, while the expression of p38γ was higher in pc-DNA-3.1 group which indicated that the transfection was successful (Fig. 2B). Fig. 2C illustrated that the protein level was also changed with the same trend to the mRNA levels in BC cell lines. MDA-MB-231 cells transfected with p38γ siRNAs could reduce OD value (450 nm), suggesting a decline in cell viability($P < 0.001$)in comparison with control group (Fig. 2D).

In addition, flow cytometry assay result for cell apoptosis was exhibited in Fig. 3A. The number of apoptosis cells in the si-p38γ group was found to be remarkably increased, which indicated that p38γ could inhibit propagation of tumor cells.

3.3. Si-p38γ suppresses breast cancer cells invasion and migration

MDA-MB-231 are human breast cancer cell line with high metastatic potential. As shown in Fig. 3B, p38γ knock out contributed to decreasing the invasive cells than control groups ($P < 0.001$) (Fig. 3B). As displayed in Fig. 3C, at 48 h, the number of migrated cell in the si-p38γ group significantly decline ($P < 0.001$).

3.4. The effect of p38γ on metabolites in MDA-MB-231 cell line

The metabolites of three groups were analysed by gas chromatography-mass spectrometer (GC–MS). A total of 238 metabolites were detected and relatively quantified, and a total of 72 metabolites expressed significantly among three groups (all $P < 0.05$, FDR < 0.05, Table 2), including 10 up-regulated metabolites such as glycero-3-Phosphocholine, adenosine and cystine et al. The down-regulated metabolites contained 6-phosphogluconic acid, docosahexaenoic acid and adenosine diphosphate et al. The relative levels of metabolites were visualized in a heat map (Fig. 4A).

Partial least square discrimination analysis (PLS-DA) was mainly used for analysis of the differences among multi-group. Each data point on the graph stands for a single sample, and the ellipse refers to the 95% confidence interval. Primary component 1 (PC1) and primary component 2 (PC2) was used for the explanation of 30.8% difference, PC1 accounted for 15.3% and PC2 accounted for 15.5% (Fig. 4B). Metabolite-metabolite correlation analysis (MMCA) was applied to analyzing the correlation in control, si-p38γ and pc-DNA-3.1-p38γ groups of MDA-MB-231 cell line (Fig. 4C). In control cells, most compounds were down-regulated in si-p38γ group, and we observed that the cluster connected by spermine and ophthalmic acid. The pink line indicated the positive correlation while the purple line indicated the negative. In

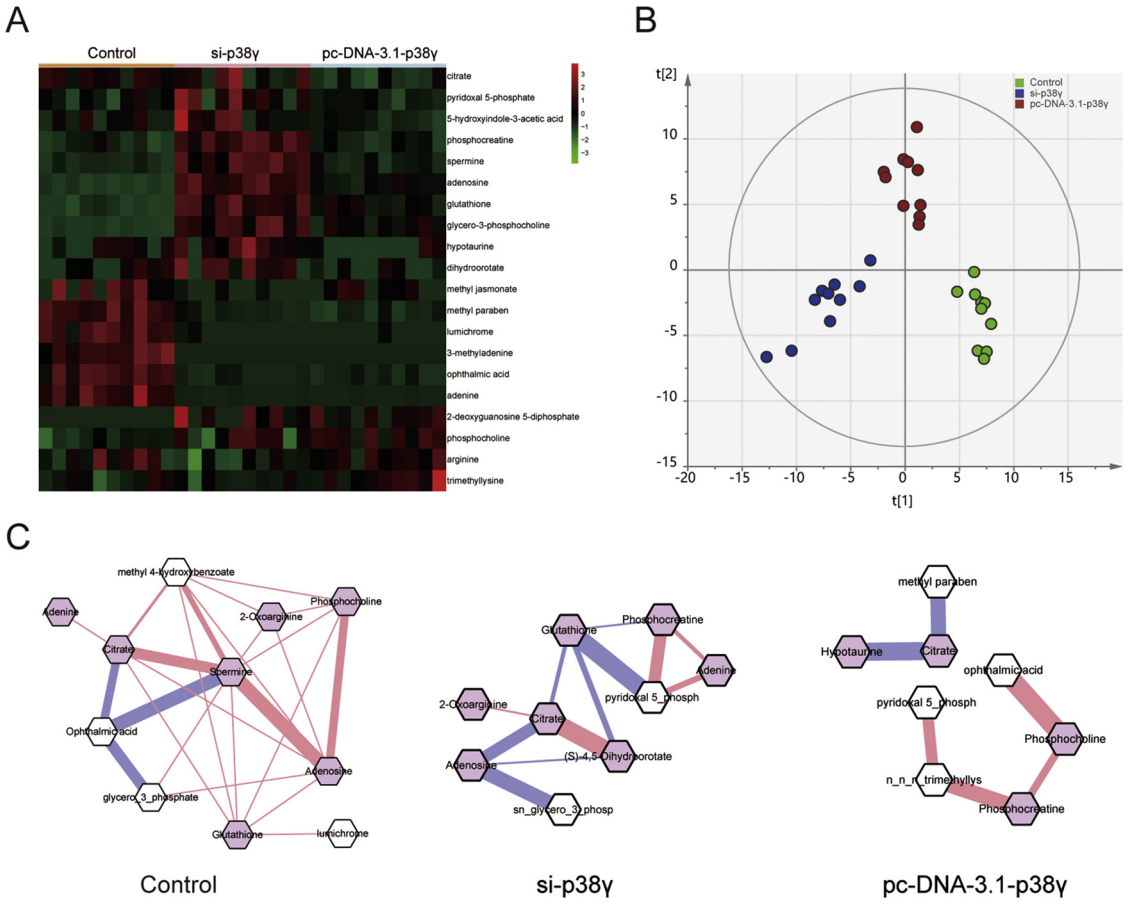

Fig. 4. Quantitative and qualitative determination of metabolites in two groups by. GC–MS.
(A)Heatmap: 20 metabolites with significant difference between three groups (*Student-t test*). (B) PLS-DA model: Control, p38γ knockdown and p38γ overexpressed groups were clearly separated. Each point represented an independent sample. (C) Metabolite-metabolite correlation analysis (MMCA) highlights differences in metabolic physiological states in control si-p38γ and pc-DNA-3.1-p38γgroup. Thickness of the edges is proportional to the magnitude of correlation coefficient and the color represents positive (pink) correlation coefficient. (For interpretation of the references to colour in this figure legend, the reader is referred to the web version of this article.)

si-p38γ group, the main correlation networks with significant differences compared to control. Si-p38γ presented a weaker correlation and amino acids or some nucleotide products. Pyridoxal and citrate were located in the connection center, which could imply that metabolic pathways involving amino and nucleotide metabolism, whose metabolites exhibited high correlations within control group, were noticeably changed in si-p38γ group. In pc-DNA-3.1-p38γ group, the main correlation network was much weaker than si-p38γ. And we can found that the citrate was all correlated negatively with other metabolites and pyridoxal was positively correlated with other metabolites.

3.5. The effect of p38γ on metabolism pathway

Metaboanalysis platform was used for enriching the metabolites in different metabolic pathways. As shown in Table 3, a total of 83 pathways included the detected metabolites and there were 27 pathways in significant enrichment (all $P < 0.05$, FDR < 0.05), including purine metabolism, intracellular signalling through adenosine receptor A2 A and adenosine, alpha linolenic acid and linoleic acid metabolism etc..

4. Discussion

The p38 MAPKs are ubiquitous signaling cascades, consisting of p38α (MAPK14), p38β (MAPK11), p38γ (MAPK12/ERK6) and p38δ (MAPK13/SAPK4) that have been involved in inflammation, cell differentiation, cell propagation, cell growth, cell death, cell senescence and carcinogenesis (Thornton and Rincon, 2009), which can transmit extracellular stress stimuli such as cytokines, ultraviolet ray (UV) exposure, osmotic shock and heat shock into target gene by regulating transcription factor. The pathway is also a promising therapeutic target for many diseases and over 20 different p38 MAPK inhibitors have been applied in clinical trials (Goldstein and Gabriel, 2005). In this study, we focused on p38γ and used a small hairpin interference RNA of p38γ to define the function of p38γ in respect of the propagation, apoptosis, metastasis and metabolism by utilizing metabolomic approach in human breast cancer cells, which is a novel perspective on tumorigenesis related with p38γ MAPK.

Our study showed that p38γ was highly expressed in human breast cancer cell, corresponding with previous studies which proved that highly expressed p38γ protein had been detected in several tumor cell lines (Pramanik et al., 2003). The previous study indicated that p38γ can be a potential target for increase hormone sensitivity for breast cancer (Qi et al., 2012). Furthermore, we investigated the role of p38γ MAPK in breast cancer motility and development by using a small hairpin (shRNA) technique to knockdown *p38γ MAPK* expression in MDA-MB 231 cells. Our result demonstrated that p38γ MAPK might be associated with tumor metastasis since si-p38γ led to significantly inhibited cell invasion and migration. A study by Fanyan Meng and Guojun Wu revealed that p38γ might be an oncogenic property-maintaining gene rather than metastasis-promoting gene in breast cancer cells (Meng and Wu, 2013). Combined with our study, p38γ MAPK was

Table 3
The Metabolites sets enrichment.

Pathway	Statistic Q	P-Value	FDR	Hits
Galactose Metabolism	78.576	1.58E-10	1.36E-08	4
Nucleotide Sugars Metabolism	72.322	3.18E-10	1.37E-08	3
Lactose Degradation	75.848	6.91E-10	1.73E-08	2
Pyrimidine Metabolism	76.938	9.02E-10	1.73E-08	2
Arachidonic Acid Metabolism	87.583	1.38E-09	1.73E-08	1
Pyruvaldehyde Degradation	87.583	1.38E-09	1.73E-08	1
Betaine Metabolism	82.561	1.41E-09	1.73E-08	2
Selenoamino Acid Metabolism	70.89	4.31E-09	4.47E-08	3
Pyruvate Metabolism	66.284	4.68E-09	4.47E-08	3
Phosphatidylcholine Biosynthesis	58.57	4.48E-07	3.85E-06	2
Spermidine and Spermine Biosynthesis	74.749	5.95E-07	4.65E-06	2
Beta-Alanine Metabolism	65.8	6.71E-07	4.81E-06	2
Pantothenate and CoA Biosynthesis	49.373	2.92E-06	1.93E-05	2
Purine Metabolism	50.943	8.17E-06	5.02E-05	6
Urea Cycle	39.727	7.57E-05	4.07E-04	3
Methionine Metabolism	33.883	0.005723	0.028952	4
Glutamate Metabolism	32.215	0.007309	0.032558	5
Glutathione Metabolism	32.303	0.007495	0.032558	3
Tryptophan Metabolism	32.456	0.007572	0.032558	3
Arginine and Proline Metabolism	31.066	0.008146	0.033358	5
Glycine and Serine Metabolism	30.586	0.010153	0.036587	4
Citric Acid Cycle	20.678	0.010581	0.036587	3
Transfer of Acetyl Groups into Mitochondria	20.678	0.010581	0.036587	3
Bile Acid Biosynthesis	29.956	0.011764	0.036587	3
Carnitine Synthesis	30.207	0.011861	0.036587	2
Porphyrin Metabolism	30.207	0.011861	0.036587	2
Alanine Metabolism	29.986	0.011912	0.036587	2

a factor for cancer metastasis although some genetic alterations were probably also required to cooperate with it to induce metastasis in breast cancer. Similarly, a suppressed migration and invasion induced by p38γ knockdown was also observed in murine 4T1 breast adenocarcinoma cells (Kukkonen-Macchi et al., 2011). Apart from the biological function related with migration and invasion, p38γ also plays an important role in propagation and apoptosis. Consistent with our study, it was reported that p38γ was positively correlated with the glioma's malignancy grade and p38γ-siRNA inhibited cell propagation meanwhile promoting apoptosis in gliomas (Yang et al., 2013). In contrast to p38α, which serves as an important negative regulator suppressing cancer cell propagation by antagonizing the JNK-c-Jun pathway (Hui et al., 2007), p38γ, as a family member of p38 as well, is likely to be a critical oncogenic factor promoting growth and progression in breast cancer.

Despite the complex detailed mechanisms of p38γ in cancer metastasis that need to be explored further, metabolic alteration was evaluated thoroughly in our study. Metabolite profiling based on GC–MS was employed to investigate the effect of p38γ knockdown on cellular metabolism as a metabolomic approach. Conventional PLS-DA demonstrated the differences between control group and si-p38γ group, and good separation between si-p38γ group and the control group were displayed in PC1 and PC2 plots of PLS-DA without any overlaps, suggesting that p38γ knockdown significantly disturbed the metabolome of MDA-MB-231 breast cancer cell. Nevertheless, PLS-DA method could not offer any insights into the interrelationships between the metabolites. Thus, metabolite-metabolite correlation analysis (MMCA) was applied so that we were able to analyze the metabolic profile in a more sophisticated way. There were many more metabolite–metabolite correlations (CC $>$ 0.8) in the control group (22 positive) than the si-p38γ group (6 positive only), suggesting that p38γ knockdown may suppress intrinsic metabolic processes to bring about the metabolic changes.

Metabolite profiling can be used to not only illuminate the individual metabolite alteration but also to provide a comprehensive insight of the altered metabolic processes induced by both external intervention and internal aberration. In this study, si-p38γ-induced metabolic perturbations were further explored at the metabolic pathways level on the basis of these different metabolites. Among the revealed pathways that were affected by si-p38γ, purine metabolism was the most differential pathway. Previous studies have revealed that purine metabolites can provide cells with the essential energy and cofactors to facilitate cell survival and propagation, other than acting as building blocks for DNA and RNA, thus fueling cancer progression (Pedley and Benkovic, 2017). Moreover, intracellular signaling through adenosine receptors, also an affected pathway in significant enrichment, were proved to be strongly relevant to different cancers, including breast cancer (Jafari et al., 2017), ovarian cancer (Jafari et al., 2017), colorectal cancer (Molck et al., 2016), non-small-cell lung cancer (Inoue et al., 2017), oral cancer (Kasama et al., 2015) etc.

In conclusion, our study verified the high expression of p38γ MAPK in breast cancer tissue and elucidated its role in cell apoptosis, invasion and migration, suggesting its potential to promote cancer metastasis. Furthermore, we evaluated the metabolism alteration caused by p38γ knockdown via si-p38γ by a novel metabolomic approach, which proved that the metabolism of MDA-MB-231 cell was significantly affected by p38γ knockdown. Deciphering the functions of p38γ MAPK involved in signaling transduction and metabolic pathways, as were preliminarily revealed in our study, may bring forth the potential to development novel therapeutic strategies for breast cancer.

Author's contribution

Research conception and design: Hongshen Chen, Xin Wang; Data analysis and interpretation: Xin Wang, Fangdong Guo; Statistical analysis: Peisong Li; Drafting of the manuscript: Hongshen Chen, Dashuai Peng; Critical revision of the manuscript: Jianjun He. Approval of the final version: All Authors.

Funding

None.

Declarations of interest

None.

Acknowledgments

None.

References

Al-Mahdi, R., Babteen, N., Thillai, K., Holt, M., Johansen, B., Wetting, H.L., et al., 2015. A novel role for atypical MAPK kinase ERK3 in regulating breast cancer cell morphology and migration. Cell Adh. Migr. 9, 483–494.
Antoniou, A., Pharoah, P.D., Narod, S., Risch, H.A., Eyfjord, J.E., Hopper, J.L., et al., 2003. Average risks of breast and ovarian cancer associated with BRCA1 or BRCA2 mutations detected in case Series unselected for family history: a combined analysis of 22 studies. Am. J. Hum. Genet. 72, 1117–1130.
Dalasanur Nagaprashantha, L., Adhikari, R., Singhal, J., Chikara, S., Awasthi, S., Horne, D., et al., 2018. Translational opportunities for broad-spectrum natural phytochemicals and targeted agent combinations in breast cancer. Int. J. Cancer 142, 658–670.
Davidson, B., Konstantinovsky, S., Kleinberg, L., Nguyen, M.T., Bassarova, A., Kvalheim, G., et al., 2006. The mitogen-activated protein kinases (MAPK) p38 and JNK are markers of tumor progression in breast carcinoma. Gynecol. Oncol. 102, 453–461.
Fan, L., Strasser-Weippl, K., Li, J.J., St Louis, J., Finkelstein, D.M., Yu, K.D., et al., 2014. Breast cancer in China. Lancet Oncol. 15 e279-89.
Goldstein, D.M., Gabriel, T., 2005. Pathway to the clinic: inhibition of P38 MAP kinase. A review of ten chemotypes selected for development. Curr. Top. Med. Chem. 5, 1017–1029.
Gonzalez-Teran, B., Matesanz, N., Nikolic, I., Verdugo, M.A., Sreeramkumar, V., Hernandez-Cosido, L., et al., 2016. p38gamma and p38delta reprogram liver metabolism by modulating neutrophil infiltration. EMBO J. 35, 536–552.
Hui, L., Bakiri, L., Mairhorfer, A., Schweifer, N., Haslinger, C., Kenner, L., et al., 2007. p38alpha suppresses normal and cancer cell proliferation by antagonizing the JNK-c-Jun pathway. Nat. Genet. 39, 741–749.
Inoue, Y., Yoshimura, K., Kurabe, N., Kahyo, T., Kawase, A., Tanahashi, M., et al., 2017. Prognostic impact of CD73 and A2A adenosine receptor expression in non-small-cell lung cancer. Oncotarget. 8, 8738–8751.

Jafari, S.M., Panjehpour, M., Aghaei, M., Joshaghani, H.R., Enderami, S.E., 2017. A3 adenosine receptor agonist inhibited survival of breast Cancer stem cells via GLI-1 and ERK1/2 pathway. J. Cell. Biochem. 118, 2909–2920.

Johnson, K.C., Miller, A.B., Collishaw, N.E., Palmer, J.R., Hammond, S.K., Salmon, A.G., et al., 2011. Active smoking and secondhand smoke increase breast cancer risk: the report of the Canadian Expert Panel on Tobacco Smoke and Breast Cancer risk (2009). Tob. Control 20, e2.

Kasama, H., Sakamoto, Y., Kasamatsu, A., Okamoto, A., Koyama, T., Minakawa, Y., et al., 2015. Adenosine A2b receptor promotes progression of human oral cancer. BMC Cancer 15, 563.

Kim, E.K., Choi, E.J., 2015. Compromised MAPK signaling in human diseases: an update. Arch. Toxicol. 89, 867–882.

Kuchenbaecker, K.B., Hopper, J.L., Barnes, D.R., Phillips, K.A., Mooij, T.M., Roos-Blom, M.J., et al., 2017. Risks of breast, ovarian, and contralateral breast Cancer for BRCA1 and BRCA2 mutation carriers. JAMA 317, 2402–2416.

Kukkonen-Macchi, A., Sicora, O., Kaczynska, K., Oetken-Lindholm, C., Pouwels, J., Laine, L., et al., 2011. Loss of p38gamma MAPK induces pleiotropic mitotic defects and massive cell death. J. Cell. Sci. 124, 216–227.

Meng, F., Wu, G., 2013. Is p38gamma MAPK a metastasis-promoting gene or an oncogenic property-maintaining gene? Cell Cycle 12, 2329–2330.

Molck, C., Ryall, J., Failla, L.M., Coates, J.L., Pascussi, J.M., Heath, J.K., et al., 2016. The A2b adenosine receptor antagonist PSB-603 promotes oxidative phosphorylation and ROS production in colorectal cancer cells via adenosine receptor-independent mechanism. Cancer Lett. 383, 135–143.

Pedley, A.M., Benkovic, S.J., 2017. A new view into the regulation of purine metabolism: the purinosome. Trends Biochem. Sci. 42, 141–154.

Pramanik, R., Qi, X., Borowicz, S., Choubey, D., Schultz, R.M., Han, J., et al., 2003. p38 isoforms have opposite effects on AP-1-dependent transcription through regulation of c-Jun. The determinant roles of the isoforms in the p38 MAPK signal specificity. J. Biol. Chem. 278, 4831–4839.

Qi, X., Tang, J., Loesch, M., Pohl, N., Alkan, S., Chen, G., 2006. p38gamma mitogen-activated protein kinase integrates signaling crosstalk between Ras and estrogen receptor to increase breast cancer invasion. Cancer Res. 66, 7540–7547.

Qi, X., Zhi, H., Lepp, A., Wang, P., Huang, J., Basir, Z., et al., 2012. p38gamma mitogen-activated protein kinase (MAPK) confers breast cancer hormone sensitivity by switching estrogen receptor (ER) signaling from classical to nonclassical pathway via stimulating ER phosphorylation and c-Jun transcription. J. Biol. Chem. 287, 14681–14691.

Schauer, N., Steinhauser, D., Strelkov, S., Schomburg, D., Allison, G., Moritz, T., et al., 2005. GC-MS libraries for the rapid identification of metabolites in complex biological samples. FEBS Lett. 579, 1332–1337.

Siegel, R.L., Miller, K.D., Jemal, A., 2016. Cancer statistics, 2016. CA Cancer J. Clin. (66), 7–30.

Smid, M., Wang, Y., Zhang, Y., Sieuwerts, A.M., Yu, J., Klijn, J.G., et al., 2008. Subtypes of breast cancer show preferential site of relapse. Cancer Res. 68, 3108–3114.

Thornton, T.M., Rincon, M., 2009. Non-classical p38 map kinase functions: cell cycle checkpoints and survival. Int. J. Biol. Sci. 5, 44–51.

Trempolec, N., Munoz, J.P., Slobodnyuk, K., Marin, S., Cascante, M., Zorzano, A., et al., 2017. Induction of oxidative metabolism by the p38alpha/MK2 pathway. Sci. Rep. 7, 11367.

Wagner, E.F., Nebreda, A.R., 2009. Signal integration by JNK and p38 MAPK pathways in cancer development. Nat. Rev. Cancer 9, 537–549.

Wishart, D.S., 2016. Emerging applications of metabolomics in drug discovery and precision medicine. Nat. Rev. Drug Discov. 15, 473–484.

Yang, K., Liu, Y., Liu, Z., Liu, J., Liu, X., Chen, X., et al., 2013. p38gamma overexpression in gliomas and its role in proliferation and apoptosis. Sci. Rep. 3, 2089.